Plant Physiol. (1995) 109: 1093–1106

Multiple Genes, Tissue Specificity, and Expression-Dependent Modulation Contribute to the Functional Diversity of Potassium Channels in *Arabidopsis thaliana*[1]

Yongwei Cao[2], John M. Ward, Walter B. Kelly, Audrey M. Ichida, Richard F. Gaber, Julie A. Anderson, Nobuyuki Uozumi, Julian I. Schroeder*, and Nigel M. Crawford

Department of Biology and Center for Molecular Genetics, University of California, San Diego, La Jolla, California 92093–0116 (Y.C., J.M.W., W.B.K., A.M.I., N.U., J.I.S., N.M.C.); and Department of Biochemistry, Molecular Biology and Cell Biology, Northwestern University, Evanston, Illinois 60208 (R.F.G., J.A.A.)

K^+ channels play diverse roles in mediating K^+ transport and in modulating the membrane potential in higher plant cells during growth and development. Some of the diversity in K^+ channel functions may arise from the regulated expression of multiple genes encoding different K^+ channel polypeptides. Here we report the isolation of a novel *Arabidopsis thaliana* cDNA (*AKT2*) that is highly homologous to the two previously identified K^+ channel genes, *KAT1* and *AKT1*. This cDNA mapped to the center of chromosome 4 by restriction fragment length polymorphism analysis and was highly expressed in leaves, whereas *AKT1* was mainly expressed in roots. In addition, we show that diversity in K^+ channel function may be attributable to differences in expression levels. Increasing *KAT1* expression in *Xenopus* oocytes by polyadenylation of the *KAT1* mRNA increased the current amplitude and led to higher levels of KAT1 protein, as assayed in western blots. The increase in KAT1 expression in oocytes produced shifts in the threshold potential for activation to more positive membrane potentials and decreased half-activation times. These results suggest that different levels of expression and tissue-specific expression of different K^+ channel isoforms can contribute to the functional diversity of plant K^+ channels. The identification of a highly expressed, leaf-specific K^+ channel homolog in plants should allow further molecular characterization of K^+ channel functions for physiological K^+ transport processes in leaves.

K^+ is a major nutrient for plants and the most abundant cation in plant cells (reviewed by Kochian and Lucas, 1988). K^+ channels have been suggested to be important for the mediation of K^+ transport in plant cells. K^+ channels contribute significantly to diverse cellular functions, including membrane potential control (Simons, 1981; Lew, 1991; Schroeder and Fang, 1991), cellular homeostasis, osmoregulation, stomatal movements, and leaf orientation (for reviews, see Moran and Satter, 1989; Schroeder and Hedrich, 1989; Schroeder et al., 1994).

At least two general classes of voltage-dependent K^+ channels exist in higher plant cells (Schroeder et al., 1987; Schroeder, 1988). Inward-rectifying potassium (K^+_{in}) channels are activated by membrane hyperpolarization and were shown to provide a pathway for low-affinity K^+ uptake and membrane potential control in guard cells (Schroeder et al., 1987; Schroeder and Fang, 1991; Fairley-Grenot and Assmann, 1993). K^+_{out} are activated by membrane depolarization and allow K^+ efflux (reviewed by Schroeder and Hedrich, 1989; Tester, 1990). Detailed studies of aleurone cells, pulvinus motor cells, mesophyll cells, root cells, suspension-culture cells, and other plant cell types have shown that either one or both of these types of K^+ channels are expressed in many plant cell types (for complete refs., see Schroeder and Hedrich, 1989; Tester, 1990; Schroeder et al., 1994). Additional classes of K^+ channels exist, such as ATP-activated K^+ channels (Spalding and Goldsmith, 1993). Further subtypes of K^+ channels within each class can be expected, since functionally diversified K^+ channels exist in animal cells. The diversity in animal K^+ channels arises from multiple genes (Chandy et al., 1990; Wei et al., 1990), alternative RNA splicing of single genes (Schwarz et al., 1988), homo- and heteromultimeric assembly of different α subunits (Isacoff et al., 1990; Rüppersberg et al., 1990), association with β subunits (Rettig et al., 1994), posttranslational modifications (Perozo and Bezanilla, 1990; Hoger et al., 1991; Drain et al., 1994), and different levels of expression (Honore et al., 1992; Moran et al., 1992). However, at present little is known about the molecular basis of K^+ channel diversity in plants.

Two closely related K^+ channel genes, *KAT1* and *AKT1*, have been isolated from *Arabidopsis thaliana* by complementation of yeast mutations affecting K^+ uptake (Anderson et al., 1992; Sentenac et al., 1992; reviewed by Sussman, 1992).

[1] This work was supported by grants from the Department of Energy (De-FG03–94-ER20148), and in part by the National Science Foundation, the Invitrogen Corporation, and the Powell Foundation to J.I.S. and in part by the National Institutes of Health (GM40672) and Powell Foundation to N.M.C, and in part by the National Science Foundation (MCB-946577) to R.F.G. Y.C. was supported by a Rockefeller Foundation fellowship.

[2] Present address: Division of Biology, 156–29, California Institute of Technology, Pasadena, CA 91125.

* Corresponding author; fax 1–619–534–7108.

Abbreviations: K^+_{in} channel(s), inward-rectifying K^+ channel(s); K^+_{out} channel(s), outward-rectifying K^+ channel(s); RFLP, restriction fragment length polymorphism; S, siemens; SSPE, 150 mM NaCl, 8 mM NaH_2PO_4, 1 mM EDTA, pH 7.4; TPBS, PBS containing 0.1% Tween 20.

One of these, *KAT1*, has been functionally identified as a first eukaryotic K^+_{in} channel by heterologous expression in *Xenopus* oocytes (Schachtman et al., 1992). The time and voltage dependencies lack of inactivation, cation selectivity, Ba^{2+} and tetraethylammonium block, and external K^+ dependence of KAT1 expressed in oocytes were demonstrated to correlate closely with the properties of K^+_{in} in higher plant cells (Schachtman et al., 1992). Furthermore, voltage-dependent Cs^+ block, results of detailed selectivity studies, and cytosolic regulation are also consistent with native plant inward K^+ channels (Hoshi, 1995; Very et al., 1995). Recent yeast expression studies have also shown expression of K^+_{in} channels by KAT1, with properties presumed (see "Discussion") to be different from oocyte studies (Bertl et al., 1995).

It is interesting that KAT1 and AKT1 genes do not show sequence or structural homology to recently cloned animal inward-rectifying K^+ channels (Ho et al., 1993; Kubo et al., 1993a, 1993b). However, plant K^+_{in} show some homology to animal outward-rectifying K^+ channels in two highly conserved regions presumably involved in voltage-sensing (S4), K^+ selectivity (H5), and the predicted membrane-spanning topology of the core region of the channel (Anderson et al., 1992; Sentenac et al., 1992). Recent studies suggest that the voltage-dependent activation of plant K^+_{in} channels can be ascribed to intrinsic gating. It was shown that K^+_{in} channel activation is not mediated by a cytosolic Mg^{2+} block mechanism (Hoshi, 1995; Schroeder, 1995). Furthermore, plant-animal chimera K^+ channels show that the N-terminal region including the KAT1 S4 sequence results in activation by hyperpolarization but not depolarization (Cao et al., 1995), which differs from animal inward-rectifying K^+ channels.

Results from animal K^+ channel studies suggest that single-site mutations in amino acid sequences among members of K^+ channel families can result in significant changes in voltage dependencies, ion selectivity, single-channel conductance, and block (for reviews, see Jan and Jan, 1992; Brown, 1993). Therefore, isolation and characterization of additional plant K^+ channel genes is important for a molecular understanding of the basic structure, physiological functions, and differential expression of K^+ channel proteins. In the present study, we report the further characterization of two previously isolated K^+ channel genes as well as the cloning and characterization of a novel gene from Arabidopsis, which is highly homologous to *AKT1* but shows a specific high expression level in leaves. The existence of multiple K^+ channel genes and the differential expression of these genes may account for part of the diverse functions of plant K^+ channels. In addition, we find that the expression level can affect the electrophysiological properties of the KAT1 K^+ channel, which provides an additional mechanism for diversifying plant K^+ channel function.

MATERIALS AND METHODS

Isolation of *KAT1**, *AKT1**, and *AKT2* Clones

PCR fragments of the KAT1 channel and an *Acc*I restriction fragment (1.6 kb) from the *KAT1* cDNA clone (Anderson et al., 1992), which contains six putative membrane-spanning segments, were radiolabeled with [^{32}P]dATP and used to screen an *Arabidopsis thaliana* cDNA library constructed in the λYES vector (Elledge et al., 1991). Hybridization was performed at low stringency in 5× SSPE, 5× Denhardt's solution, and 50 mg/mL sheared salmon sperm DNA at 47°C for 48 h. Filters were washed twice in 4× SSPE, 0.5% (w/v) SDS for 30 min each at 47°C, followed by two washes for 15 min each in 1× SSPE, 0.5% (w/v) SDS at 47°C. The positive phage clones were converted into plasmid clones in vivo by using the cre-lox recombination system (Elledge et al., 1991). All inserts were then subcloned into pBluescript KS II vector (Stratagene) and sequenced using the United States Biochemical Sequenase kit. Sequence analysis and alignment were performed with PCGENE computer software (IntelliGenetics Inc., Zurich, Switzerland).

To isolate an *AKT2* genomic clone, an *A. thaliana* genomic DNA library was constructed (Wilkinson and Crawford, 1991) in a λDASH vector (Stratagene). The partial AKT2 cDNA clone isolated from the above-mentioned λYES library was used as a probe to screen this genomic DNA library at high stringency. The hybridization and washing conditions were the same as described above except a higher temperature (65°C) was used. Inserts harbored in positive phages were excised with various restriction enzymes and rehybridized with the partial *AKT2* cDNA. A 3-kb *Xba*I fragment was found to hybridize to the 5′ end of the partial *AKT2* cDNA. This fragment was further sequenced to confirm that it overlaps with the cDNA clone and was found to contain the complete 5′ coding sequence, which was absent in the partial AKT2 cDNA clone.

To remove an intron in the 3-kb *Xba*I genomic fragment and to construct a full-length *AKT2* cDNA clone with a complete coding sequence, the genomic fragment was first digested with *Kpn*I and then filled in with T4 DNA polymerase. The *Kpn*I site (GGATCC) is at the 5′ border of the intron. The resulting genomic fragment (from 5′ *Xba*I to *Kpn*I site) was then ligated to a PCR fragment amplified with a forward primer (5′-GTGCTGGGAATTTTATA-3′) at nucleotide position 228 to 244 and a reverse primer (5′-ACCATTTCAATAGTGTT-3′) at position 855 to 871. The ligation product was digested with *Xho*I and then ligated to the partial cDNA clone at the *Xho*I site (at nucleotide position 607). The entire PCR fragment was resequenced to ensure identity with the genomic coding sequence.

Oocyte Expression and Recording

KAT1 and *KAT1** cDNAs were subcloned into the *Xho*I site and *AKT2* was subcloned into the *Hin*dIII and *Xba*I sites of the pBluescript KS II vector. *KAT1+poly(A)* was constructed by cloning the *KAT1* cDNA into the *Xho*I site of a modified pBluescript KS vector (gift of C. Labarca, California Institute of Technology, Pasadena) in which a poly(A)$^+$ segment (50 adenine nucleotides) was inserted between the *Apa*I and the *Kpn*I sites. Capped mRNA was transcribed from linearized plasmids in vitro using T7 RNA polymerase and an RNA transcription kit (Stratagene). *Xenopus laevis* oocytes were isolated as described by

Cao et al. (1992) and injected with 10 ng of mRNA in 50 nL of water. Oocytes were incubated in regular Barth's solution (88 mM NaCl, 1 mM KCl, 2.4 mM $NaHCO_3$, 10 mM Hepes-NaOH, 0.33 mM $Ca[NO_3]_2$, 0.41 mM $CaCl_2$, 0.82 mM $MgSO_4$, pH 7.4) supplemented with 50 μg/mL gentamycin for 1 to 3 d before recording.

Ionic currents were recorded using two-electrode voltage clamping. Voltage-pulse protocols, data acquisition, and data analysis were performed on an 80386-based microcomputer using the program PCLAMP (Axon Instruments, Inc., Foster City, CA) and a Cornerstone model TEV-200 voltage-clamp amplifier (Dagan Corp., Minneapolis, MN). Voltage and current microelectrodes were filled with 3 M KCl and had resistances of less than 2 MΩ. All experiments were carried out at room temperature. Data were low-pass filtered with an eight-pole Bessel filter. Membrane currents as well as clamped oocyte membrane potentials were recorded simultaneously on two separate channels for monitoring of time resolution and for later analysis. Leakage currents were subtracted using digital depolarizing P/4 and P/6 linear leakage subtraction methods (Bezanilla and Armstrong, 1977; Schachtman et al., 1992). Control experiments without leakage subtraction were performed to ensure that a linear background conductance was subtracted. Membrane currents were measured in a K^+ Ringer's solution that contained 117 mM KCl, 1.8 mM $CaCl_2$, 1 mM $MgCl_2$, 10 mM Hepes, pH 7.4.

Oocyte Membrane Protein Isolation and Western Blot Analysis

Microsomal membrane protein was isolated from oocytes using the procedure of Corey et al. (1994) with modifications. Oocytes were homogenized in 0.32 M Suc, 50 mM Tris-Cl, pH 7.5, 1 mM EDTA, and 1 mM PMSF in a Dounce homogenizer at 4°C. The homogenate was centrifuged for 10 min at 250*g*, and the membranes were then pelleted at 25,000 rpm in a Beckman SW27 rotor for 40 min at 4°C. The membranes were suspended in water, and protein concentration was determined by the bicinchoninic acid assay method (Pierce). Protein samples were then precipitated with 10% (w/v) TCA and boiled for 5 min in sample buffer (Laemmli, 1970).

Oocyte membrane proteins were separated on 10% SDS polyacrylamide gels (Laemmli, 1970) and transferred to Immobilon-P polyvinylidene difluoride membranes (Millipore) for 1 h at 100 V. Transfer membranes were blocked for 1 h in PBS containing 1% BSA, 5% (w/v) dry milk, and 1 M Gly and washed in TPBS. The blots were immunostained as previously described (Ward et al., 1992). Antibodies were diluted in TPBS containing 1% (w/v) dry milk. Blots were incubated with polyclonal rabbit antisera against KAT1-glutathione *S*-transferase fusion protein (1:1000 dilution), washed in TPBS, and incubated with goat anti-rabbit IgG conjugated to alkaline phosphatase. After the blots were washed, they were developed by incubation with 5-bromo-3-chloro-3-indoyl phosphate and nitroblue tetrazolium.

Complementation Test in Yeast

Because the *KAT1** and *AKT1** cDNAs, isolated here, were inserted in the pSE936 vector (excised from λYES phage, see Elledge et al., 1991) in the wrong orientation for expression in yeast, the *KAT1** and *AKT1** cDNAs, as well as the constructed full-length *AKT2* cDNA, were resubcloned into the *Xho*I site of the pSE936 vector. This vector contains the Gal-inducible GAL1 promoter and the URA3-selectable marker. The *Saccharomyces cerevisiae* mutant strain CY162, *MATa ura3–52 trk1Δ his3Δ200 his4–15 trk2Δ1*::pCK64 (Anderson et al., 1992), was transformed as previously described (Dohmen et al., 1991). Transformants were first selected for uracil prototrophy on medium consisting of 0.67% (w/v) yeast nitrogen base and 2% (w/v) agar supplemented with 100 mM KCl, 2% (w/v) Glc, and all amino acids except uracil. Colonies were then plated on a similar medium at 30°C in which 100 mM KCl and 2% (w/v) Glc were replaced with 2% (w/v) Gal and 2% (w/v) Suc. Plasmid DNA in selected yeast transformants was rescued in *Escherichia coli* and rechecked by restriction enzyme digestion to make sure that all yeast transformants harbored the appropriate plasmid.

DNA and RNA Gel Blot Analysis and RFLP Mapping

Genomic DNA and poly(A)$^+$ mRNA preparations were carried out as described by Tsay et al. (1993). Southern and northern blot analyses were carried out under stringent hybridizations conditions (42°C with 50% formamide) as described by Tsay et al. (1993) to eliminate any cross-hybridization among *KAT1*, *AKT1*, and *AKT2*. ^{32}P-labeled *KAT1*, *AKT1*, and *AKT2* probes were synthesized using random primers and Klenow DNA polymerase and had a specific activity of 5×10^8 to 1×10^9 cpm/μg DNA. RFLP mapping was performed as described by Chang et al. (1988) using genomic DNAs isolated from a cross between Landsberg *erecta* and Columbia ecotypes. These genomic DNAs were digested with *Eco*RI, *Bgl*II, *Hin*dIII, and *Xba*I and were then probed with the *AKT2* λDASH genomic clone to reveal DNA polymorphisms between Landsberg and Columbia. RFLP mapping data were analyzed using the MAPMAKER computer program developed by Lander et al. (1987) and modified for Macintosh computers by Les Proctor (DuPont).

RESULTS

Isolation of K^+ Channel cDNA Clones from Arabidopsis

To identify additional K^+ channel clones in Arabidopsis, a partial *KAT1* cDNA (Anderson et al., 1992) and PCR products, which encode the hydrophobic core region, were used to screen an *A. thaliana* cDNA library at reduced stringency. From 5×10^4 plaques screened, 12 candidate clones were isolated. Restriction digestion and subsequent sequence analysis showed that these clones were derived from at least three different mRNA species. Two previously identified clones, *KAT1* and *AKT1* (Anderson et al., 1992; Sentenac et al., 1992), and a third, novel sequence were isolated, which is most similar to *AKT1* (see below)

and was thus designated as *AKT2*. The *KAT1* and *AKT1* cDNA clones isolated here (*KAT1** and *AKT1**) were both longer than the published clones, because of the presence of long poly(A)$^+$ tails at the 3′ end of the *KAT1** and *AKT1** clones and an additional 74 nucleotides at the 5′ end of the *AKT1** clone (Fig. 1). The additional 5′ sequence does not contain an in-frame start codon. Thus, the coding sequence of the proteins encoded by *KAT1* and *KAT1**, or *AKT1* and *AKT1**, are identical.

Polyadenylation of the *KAT1* mRNA Increases the Expression Level and Changes the Biophysical Properties of the KAT1 Channel

It has been reported that the plant *KAT1* cDNA can be expressed in *Xenopus* oocytes and that KAT1 expresses the hallmark macroscopic properties of higher plant K^+_{in} channels (Schachtman et al., 1992). To test whether the *KAT1** cDNA clone isolated here would function in *Xenopus* oocytes, *KAT1** was first subcloned into a transcription vector and then capped sense mRNA transcripts were synthesized in vitro and injected into oocytes. The oocyte membrane was voltage clamped at −40 mV and then stepped for 1.5-s intervals to both depolarized and hyperpolarized potentials. An inward-rectifying K^+ current was recorded in *KAT1**-injected oocytes (n = 134 oocytes) (Fig. 2a) but not in uninjected oocytes (Schachtman et al., 1992). The current induced by *KAT1** injection had properties similar to the current induced by *KAT1* injection. Both currents were activated by hyperpolarization, showed no inactivation or activation by depolarization, and displayed the previously reported selectivity sequence among monovalent cations ($K^+ > NH_4^+ > Rb^+ \gg Na^+ \approx Li^+ \geq Cs^+$) (Schachtman et al., 1992; Very et al., 1995). Ammonium current amplitudes at −120 mV had approximately 28% of the magnitude of K^+ current amplitudes, confirming the previously published current amplitude ratio after correction for background currents of KAT1 expressed in oocytes

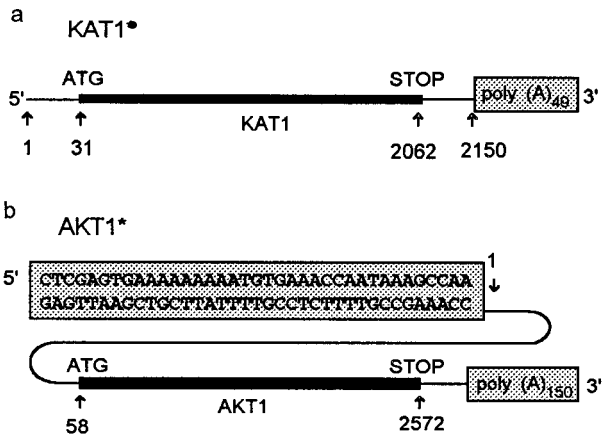

Figure 1. Schematic representation of *KAT1** and *AKT1** cDNA clones. *KAT1** (a) and *AKT1** (b) sequences that are in addition to the published *KAT1* and *AKT1* sequences are shown in shaded boxes. The numbers shown above or below arrows indicate nucleotide positions based on the published sequences. The open reading frame of *KAT1* and *AKT1* are represented by thick bars.

(Schachtman et al., 1992) but differing from NH_4^+ selectivities estimated from KAT1 expression in yeast (Bertl et al., 1995).

The *KAT1** cDNA isolated here expressed more rapidly in oocytes, and the resultant current was larger than *KAT1*. K^+ current could be easily detected in oocytes 10 h after *KAT1** mRNA injection, and this current rapidly increased within 24 h to more than 5 μA at test potentials of −120 mV (Fig. 2, a and b). In contrast, *KAT1*-injected oocytes did not develop detectable current until 24 h after injection, and the current rarely exceeded 1 μA at −120 mV even after 3 d of incubation (Fig. 2b).

Differences in biophysical properties of KAT1- and KAT1*-induced currents were also observed. KAT1* current showed activation at potentials negative to −60 mV as determined by an increase in conductance at more negative membrane potentials ("inward rectification"). This threshold potential for activation was approximately 30 mV more positive than the threshold of activation for KAT1 (Fig. 2b). To determine whether this shift in activation potential reflected a change in the voltage dependence or whether it could be attributed to current resolution in oocytes, slow hyperpolarizing voltage ramps were applied to *Xenopus* oocytes. In the membrane potential range from −10 to −50 mV, *KAT1**-injected, *KAT1*-injected, and noninjected control oocytes showed similar background conductances of 2 to 5 μS and no significant K^+ channel activity (Fig. 2, c and d). The hyperpolarization-induced activation during slow voltage ramps produced clearly measurable differences in the activation potentials of *KAT1**- and *KAT1*-injected oocytes (Fig. 2, c and d). Slow hyperpolarizing voltage ramps displayed an approximately +30 mV shift in the activation potential of *KAT1** when compared to *KAT1* (Fig. 2, c and d). The differences in activation potential did not depend on the speed of voltage ramps, because much slower ramps gave similar results. The difference in the threshold potential was not due to a scaling factor effect as determined in control experiments with a K^+_{out} gene from *Xenopus* (*XSha2*; Ribera, 1990) expressed in oocytes. The threshold potential could be resolved at low current amplitude and did not shift significantly when expression levels increased by more than 10-fold (measured at −10 mV test potentials) by injecting different amounts of mRNA (Fig. 2e). In addition, the rate of activation, measured as the rise time to 50% of maximum current for voltage step pulses to −120 mV from a holding potential of −40 mV, was more rapid for KAT1* (169 ± 50 ms, n = 21) than for KAT1 (280 ± 43 ms, n = 14). These observations suggest that the shift in activation potential reflects a change in voltage dependence.

Since *KAT1** and *KAT1* differ only at the end of the 3′ untranslated region, where *KAT1** was missing the final 11 untranslated nucleotides but had a 49-bp-long poly(A)$^+$ tail instead (Fig. 1a), it is likely that the differences in current amplitudes, activation thresholds, and half-activation times were due to the polyadenylation of the *KAT1** transcript. To test this hypothesis, we subcloned the *KAT1* cDNA into a transcription vector that had 50 adenine nucleotides inserted downstream of the cloning site (see "Materials and Methods") and then synthesized mRNA in

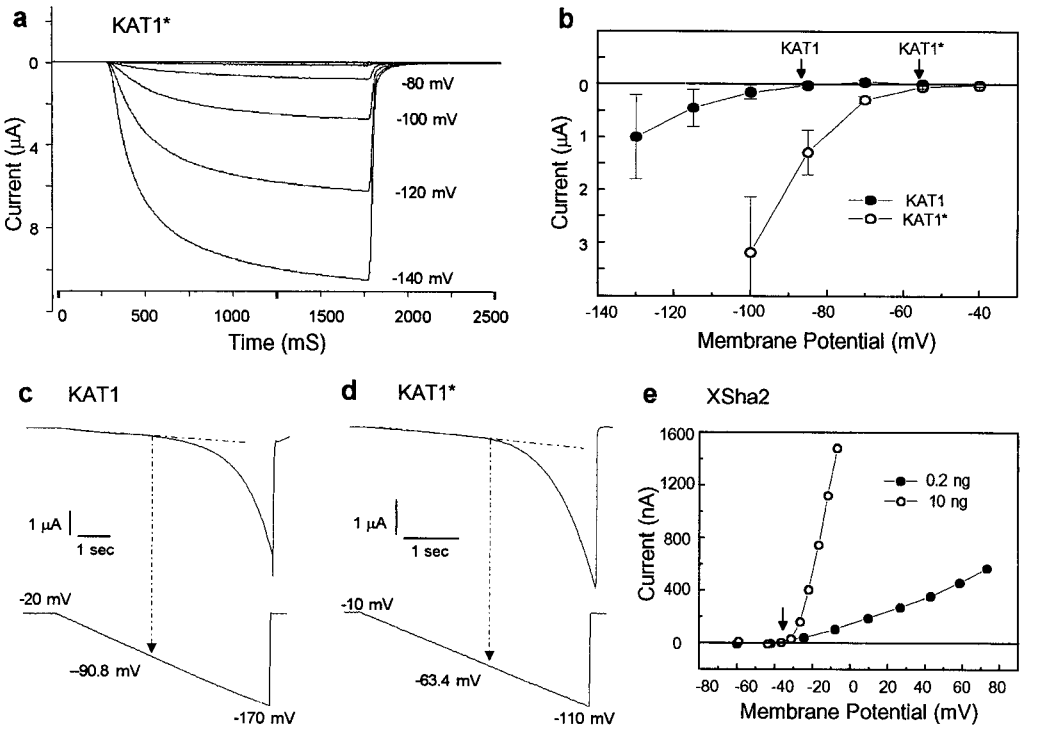

Figure 2. Expression of *KAT1** and *KAT1* in *Xenopus* oocytes. a, Voltage-clamp recording of a *KAT1**-injected oocyte. Inward currents (downward deflections) in response to hyperpolarizing voltage steps are shown. The membrane potential was held at −40 mV and stepped for 1.5 s to test potentials ranging from −60 to −140 mV in −20-mV increments as indicated to the right of recorded currents. b and e, Current-to-voltage relationships. Whole-cell currents in oocytes injected with *KAT1* or *KAT1** (10 ng each) (b) or *XSha2* (0.2 or 10 ng) (e) are plotted as a function of membrane potential. Currents were measured at the end of 1.5 s of stimulation after subtraction of linear background currents. The threshold potentials where currents show rectification are indicated by arrows. Vertical lines in b indicate the SD in measurements taken from *KAT1*-injected (n = 7) and *KAT1**-injected (n = 11) oocytes. c and d, Inward currents induced by slow hyperpolarizing voltage ramps in *KAT1*-injected (c) and *KAT1**-injected (d) oocytes. The voltage-ramp protocols are shown below the corresponding current traces. The threshold potentials where currents show rectification are indicated by arrows. Currents were recorded 1 d (*KAT1**, *XSha2*) or 3 d (*KAT1*) after mRNA injection.

vitro. Oocytes injected with this modified *KAT1* mRNA showed a current almost identical with the KAT1* current (Fig. 3a), with a threshold of activation at approximately −60 mV (Fig. 3b) and a half-activation time of 181 ± 52 ms (n = 9) at −120 mV.

It is possible that the polyadenylation of the *KAT1* transcript increases protein expression levels in oocytes. To test this hypothesis, western blot analysis was performed using a polyclonal antibody raised against a KAT1-glutathione *S*-transferase fusion protein. Anti-KAT1 antibodies reacted with several protein bands in uninjected oocytes (Fig. 4a, lane 1). These background immunostaining bands were not close to the predicted molecular mass of KAT1 of 78 kD (Anderson et al., 1992) and thus did not interfere with the analysis of KAT1 expression using western blots. KAT1 protein was not detected in lanes containing 1, 10, or 40 μg of oocyte membrane protein from oocytes injected with *KAT1* mRNA (Fig. 4a, lanes 2–4). However, KAT1 protein (74 kD) was detected in lanes containing either 10 or 40 μg of membrane protein from oocytes injected with *KAT1** mRNA (Fig. 4a, lanes 6 and 7) but not in lanes containing 1 μg of oocyte protein (Fig. 4a, lane 5). When 3-fold higher amounts of *KAT1* mRNA were injected (Fig. 4b, lane 1), compared to KAT1*-injected oocytes (Fig. 4b, lane 2), KAT1 protein was detected only in KAT1*-injected oocytes. Injection of even higher amounts of KAT1 mRNA (≥25 ng) also allowed detection of KAT1 protein with anti-KAT1 antibody (data not shown). Reaction of the polyclonal antibody with KAT1 protein was confirmed by its reaction with the in vitro translated KAT1 protein (Fig. 4b, lane 4) at 73 kD, which was not detected in control translation reactions (Fig. 4b, lane 3). Differences in mobility of KAT1 protein expressed in oocytes or produced by in vitro translation are expected to be due to secondary protein modifications such as glycosylation, which would not be made in vitro under the conditions used in this study. These results indicate that polyadenylation of the *KAT1* transcript increases the expression of KAT1 protein in oocytes. Furthermore, activation properties of KAT1 depend on the level of channel proteins expressed in the plasma membrane, thus providing a posttranslational mechanism that can contribute to plant K^+ channel diversity.

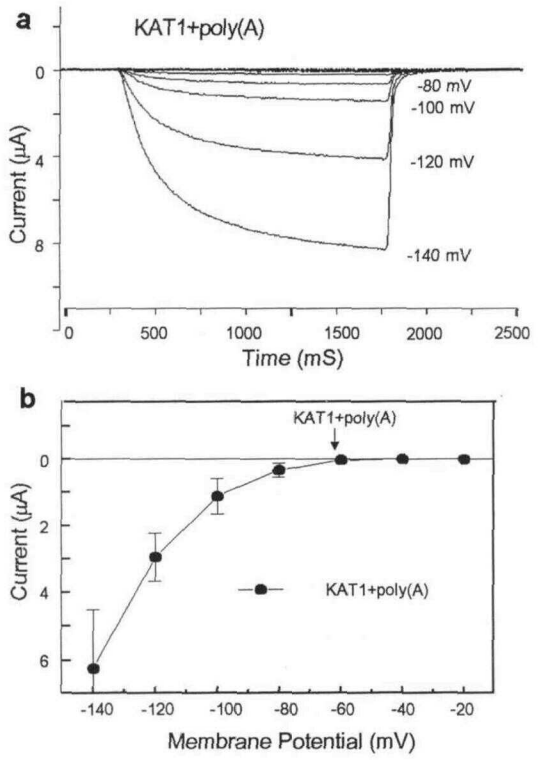

Figure 3. Expression of *KAT1+poly(A)* in *Xenopus* oocytes. Whole-cell currents (a) and the current-to-voltage relationship (b) are shown for *KAT1+poly(A)*-injected oocytes. The arrow and vertical lines in b indicate the threshold potential for activation and the SD (n = 8), respectively.

Structural Features of a Novel K^+ Channel Homolog, *AKT2*

Further diversity in plant K^+ channel function may be attributed to multiple genes encoding K^+ channels. In addition to the previously described *KAT1* and *AKT1* cDNAs, a third putative K^+ channel cDNA, *AKT2*, was isolated from an Arabidopsis λYES cDNA library. The deduced open reading frame from the initial *AKT2* cDNA clone consisted of 690 amino acids but was apparently incomplete at the amino-terminal end of the derived protein. Since we were unable to isolate cDNAs to complete the open reading frame, we isolated the corresponding genomic DNA by screening an Arabidopsis genomic DNA library. A 3-kb *Xba*I restriction fragment, which hybridized with the N-terminal coding region of the *AKT2* cDNA, was isolated from the genomic library. The combined genomic and cDNA sequences are shown in Figure 5a. A potential promoter region (TATA box, Joshi, 1987) was identified. An intron (Fig. 5a, lowercase letters) was also found in the genomic clone based on several criteria: (a) stop codons were identified in all three forward reading frames within the intron sequence, (b) splice junction consensus sequences (Hanley and Schuler, 1988) could be found at both the 5′ border and the 3′ border of the intron, and (c) the deduced amino acid sequence after removal of the intron could be well aligned to the *KAT1* and *AKT1* sequences. For subsequent functional analysis of AKT2, we constructed a cDNA clone containing all of the protein-coding region by removing the intron and then ligating the genomic sequence to the partial cDNA clone (see "Materials and Methods"). The open reading frame derived from the combined genomic/cDNA sequences consists of 802 amino acid residues with a calculated molecular mass of 91.3 kD. A second putative translation initiation codon is present within this open reading frame at nucleotide position 46 (Fig. 5a), but the first ATG is theoretically favored to serve as a start codon for translation because it is preceded by a strong ribosomal recognition site for initiation of translation, 5′-AAAATGA-3′ (Kozak, 1989). The deduced protein

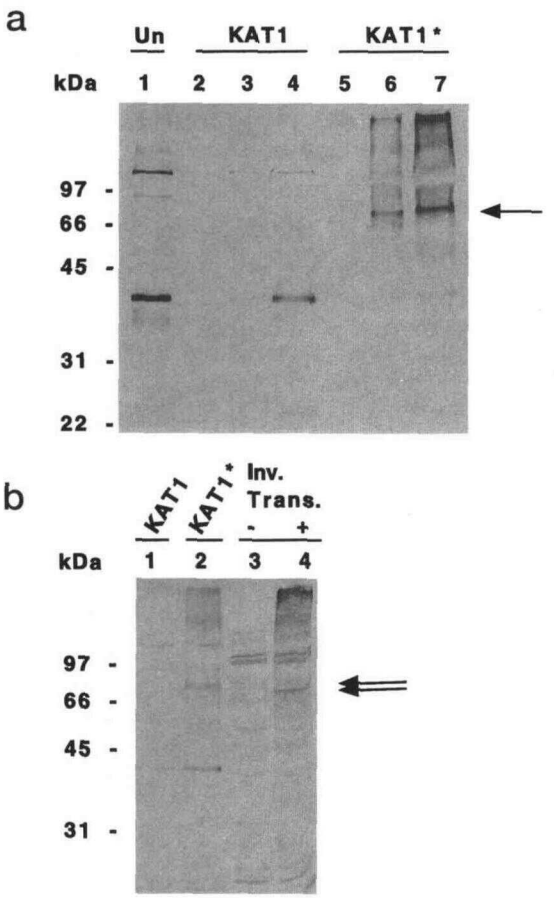

Figure 4. *Xenopus* oocytes express higher levels of KAT1 protein following injection of transcript from *KAT1** when compared to *KAT1*. a, Lane 1, 60 μg of protein from uninjected oocytes (Un). Oocytes were injected with mRNA (2.5 ng each) transcribed from *KAT1* (lanes 2–4) or *KAT1** (lanes 5–7). Oocyte membrane protein was isolated after 4 d. Lanes 2 and 5 contain 1 μg of protein, lanes 3 and 6 contain 10 μg of protein, and lanes 4 and 7 contain 40 μg of oocyte membrane protein. The arrow indicates the position of KAT1 protein at 74 kD. b, Oocytes were injected with *KAT1* mRNA (8.5 ng each, lane 1) or *KAT1** mRNA (2.5 ng each, lane 2). Oocyte membrane protein was isolated after 2 d and 40 μg of oocyte membrane protein was loaded in lanes 1 and 2. In vitro translation reaction (Inv. Trans.) without (lane 3) and with (lane 4) *KAT1* template. The arrows indicate the position of KAT1 expressed in oocytes (74 kD) and the in vitro translated KAT1 protein (73 kD).

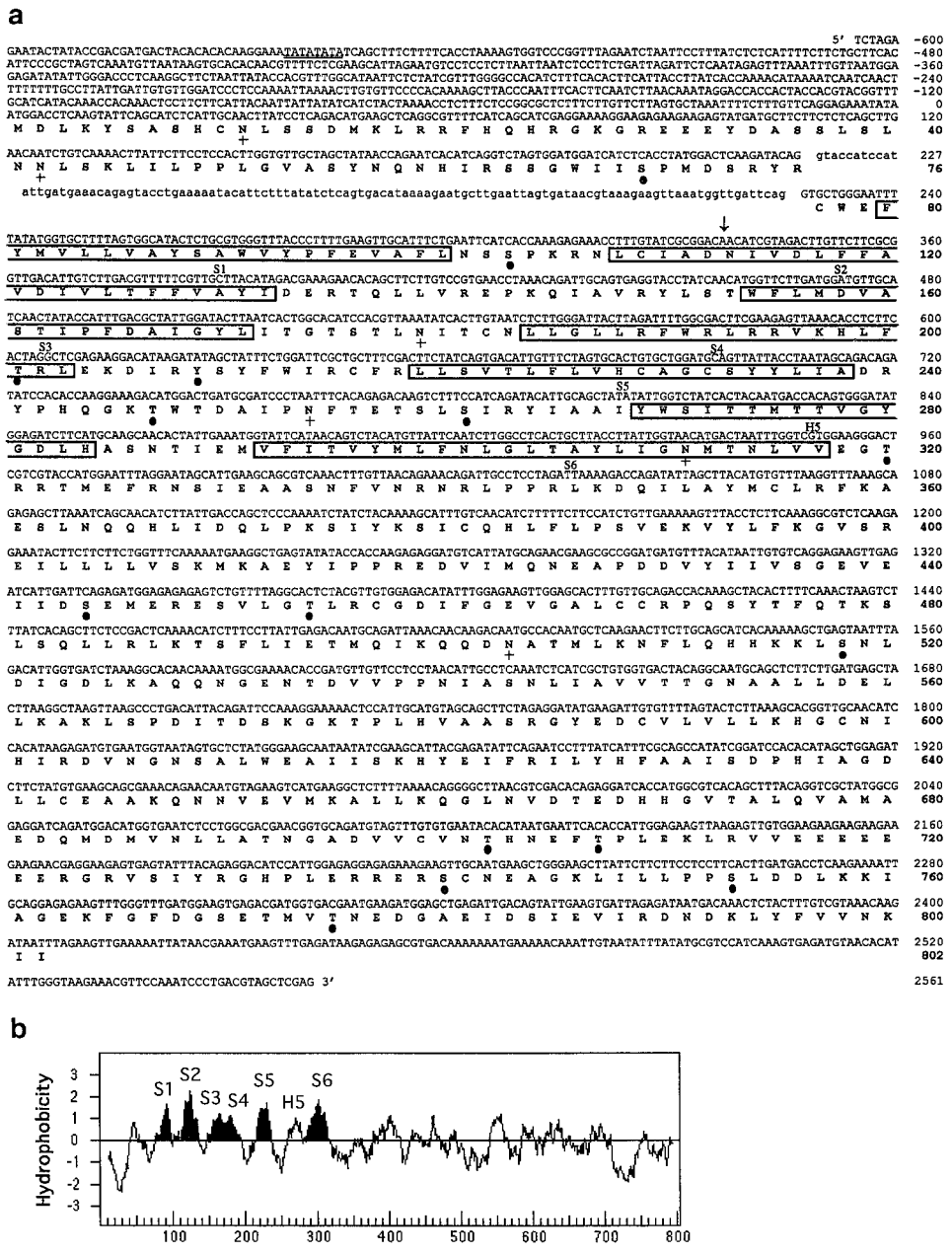

Figure 5. Sequence of the *AKT2* cDNA and hydropathy plot of the AKT2 protein. a, Nucleotide sequence of the *AKT2* gene composed of a genomic clone and a partial cDNA clone and predicted amino acid sequence of the AKT2 product. The cDNA clone starts at the position of the arrow. The intron sequence, which was removed during the construction of a full-length cDNA clone, is shown in lowercase letters and is not numbered. Additional intron sequences are present in the *AKT2* genomic sequence and are not shown here. The putative promoter sequence is underlined. Putative membrane-spanning segments (S1–S6) and the H5 region are indicated by boxes. Potential *N*-glycosylation sites (+) and phosphorylation sites (●) are marked under the corresponding amino acids. b, Hydropathy profiles of the AKT2 protein, as determined by the method of Kyte and Doolittle (1982), using a window of 19 amino acid residues. The putative membrane-spanning segments (S1-S6) and the channel pore region (H5) are indicated.

contains 6 potential *N*-glycosylation sites and 15 potential phosphorylation sites for protein kinases (Fig. 5a).

Hydropathy analysis of the deduced AKT2 polypeptide sequence revealed six possible membrane-spanning segments (S1–S6, Fig. 5, a and b), a profile very similar to the KAT1 and AKT1 proteins (Anderson et al., 1992; Sentenac et al., 1992). Sequence comparison within the hydrophobic regions of different families of channels revealed that the AKT2 protein is very similar to the KAT1 and AKT1 channels, and to a lesser extent to *Eag* (a *Drosophila* outward-rectifying K^+ channel, Warmke et al., 1991), cyclic nucleotide-gated channels (Kaupp et al., 1989), and the *Shaker*

family of K^+ channels (Tempel et al., 1987; Wei et al., 1990) (Table I).

Two highly conserved and functionally important domains in animal outward-rectifying K^+ channels, namely the voltage-sensing domain (S4), which is characterized by the presence of five to seven positively charged amino acids with each one seperated by two or three hydrophobic residues (Fig. 6a), and the K^+-selective pore-forming domain (H5) with a consensus sequence of TMTTVGYGD (residues 274–282, Fig. 5a), are also present in the *AKT2* sequence.

Similar to KAT1 and AKT1 proteins, the AKT2 protein has a region between amino acids 415 and 498 that is homologous to cyclic nucleotide-binding domains present in many other proteins, including the *Eag* channel (Warmke et al., 1991), cyclic nucleotide-gated channels (Kaupp et al., 1989), and the catabolite gene activator protein of *E. coli* (Weber and Steitz, 1984) (Fig. 6b).

There are five imperfect repeats of 32 to 33 amino acids downstream of the cyclic nucleotide-binding domain of the AKT2 protein (Fig. 6c). Each repeat has the characteristic of an ankyrin repeat, a-33 amino acid motif that usually appears in multiple copies in ankyrin proteins and ankyrin repeat-containing proteins (Lux et al., 1990; Zhang et al., 1992). The ankyrin repeat domain may mediate the localization of channel proteins or regulation of channel functions by binding to cytoskeletal elements or other proteins (Baines, 1990; Bennett, 1992). Similar repeats have been reported for the AKT1 sequence (Sentenac et al., 1992) but not for the KAT1 sequence. Thus, AKT2 is structurally more similar to AKT1, and the ankyrin repeats in plant K^+ channels (Sentenac et al., 1992; Fig. 6c) are unlikely to be a result of cDNA rearrangements.

The *AKT2* and *AKT1* mRNAs Are Differentially Expressed

To determine the expression pattern of K^+ channel genes in higher plants, high-stringency RNA blot hybridizations were carried out using poly(A)$^+$ mRNA from root and leaf tissues of young Arabidopsis seedlings. Figure 7 shows that the *AKT2* mRNA is highly expressed in leaf tissues and not in root tissues. The size of the hybridized band in leaves was approximately 2.8 kb, close to the size of the constructed *AKT2* cDNA clone (2586 bp without 5′ untranslated sequence, see Fig. 5a), indicating that the *AKT2* gene is not a pseudogene and that the constructed cDNA clone is probably a full-length clone. In contrast, *AKT1* mRNA was slightly larger than *AKT2* mRNA and was highly expressed in root tissues (Fig. 7). The *KAT1* probe, which had a specific radioactivity similar to that of the *AKT1* and *AKT2* probes and was used successfully in initial library screenings and Southern blot hybridizations, did not detect any signal on RNA blots (data not shown). These results appear to differ from the reported expression of KAT1 mRNA in shoots and roots (Kochian et al., 1993). Our results indicate that the expression of *KAT1* is low, restricted to specialized cell types of lower abundance, or developmentally regulated. Thus *AKT2* is highly expressed in leaves and differentially expressed with respect to *AKT1* and *KAT1*.

AKT2 Gene Is Located on Chromosome 4

DNA gel blot analysis of two ecotypes of Arabidopsis genomic DNAs cleaved with various restriction enzymes revealed several bands hybridizing with the *AKT2* cDNA probe (Fig. 8). The band pattern is consistent with the restriction map of AKT2 genomic clones. The bands shown in Figure 8 indicate that probably one gene encoding the *AKT2* protein is present in Columbia and Landsberg genomes. In an attempt to establish whether *AKT2* is closely linked to a known mutation, we determined the genetic map position of *AKT2* using RFLP mapping (Chang et al., 1988). Genomic DNA blot hybridizations with an AKT2 λDASH genomic clone as a probe revealed an *Xba*I polymorphism between Columbia and Landsberg (data not shown) and 106 individuals were scored and analyzed. *AKT2* was localized to the center of chromosome 4 between *Agamous* and *Cer2* markers (Fig. 9).

Functional Test of *AKT2* cDNA in Yeast and *Xenopus* Oocytes

S. cerevisiae mutants in which two K^+ transport systems (*TRK1* and *TRK2*) are deleted have been constructed (Ramos et al., 1985; Ko and Gaber, 1991). Yeast cells, like plant cells, contain a proton-extruding ATPase in the plasma membrane that provides the driving force for K^+ uptake. Therefore, expression of K^+_{in} from plants rescues

Table I. *Percentage of identical amino acids in analogous positions within the region spanning from S1 through S6 between pairs of different channels*

The percentages of identical amino acids within the entire hydrophobic core region (S1–S6) were calculated for each pair of channels using PCGENE software (IntelliGenetics, Inc.).

	AKT1	*KAT1*	*Eag*	*cGMP*	*Shal*	*Shaw*	*Shab*	*Shak*
AKT2	59	60	29	21	20	16	14	16
AKT1		63	30	25	19	18	19	17
KAT1			28	23	17	17	17	16
Eag				23	20	17	17	17
cGMP					18	15	14	15
Shal						39	38	43
Shaw							43	45
Shab								45

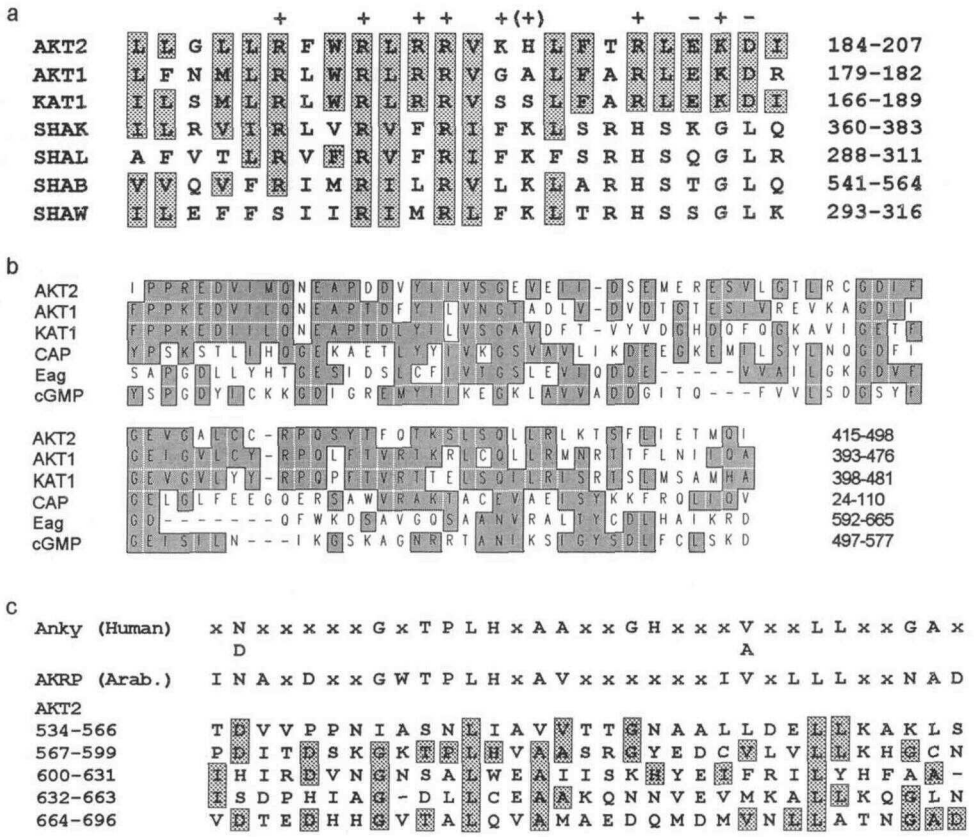

Figure 6. Amino acid sequence alignment within the S4 segment, cyclic nucleotide-binding domain, and ankyrin repeat domain. a and b, Amino acid sequences of the S4 segment and the putative cyclic nucleotide-binding domain of *AKT2* were aligned with the corresponding regions of other proteins. Positively charged (+) and negatively charged (−) amino acids in the S4 segment of *AKT2* are indicated. Amino acids that are identical with or similar to the *AKT2* S4 sequence (a) or conserved among at least three cyclic nucleotide-binding domains (b) are boxed and shaded. Gaps (shown as dashes) were introduced for optimal alignments. c, The ankyrin-like repeats of *AKT2* were aligned with the consensus sequences from the human erythrocyte Anky cDNA (Lux et al., 1990) and from the Arabidopsis (Arab.) AKRP cDNA (Zhang et al., 1992). An "x" in consensus sequences marks a position where no consensus exists. Amino acids that are identical with either of the consensus sequences are shaded. Gaps (shown as dashes) were introduced for optimal alignments.

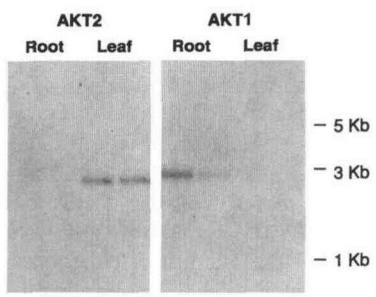

Figure 7. *AKT1* and *AKT2* mRNAs are differentially expressed in roots and leaves. Two separate preparations of poly(A)$^+$ mRNAs from root and leaf tissues of Arabidopsis seedlings were loaded on the gel (1 mg per lane) and hybridized with ^{32}P-radiolabeled *AKT1* or *AKT2* cDNA as indicated.

these yeast mutants, which has been demonstrated for KAT1 and AKT1 channels (Anderson et al., 1992; Sentenac et al., 1992). To test whether the cDNA clones isolated here would complement the yeast mutant, *KAT1**, *AKT1**, and *AKT2* cDNAs were subcloned into a yeast expression vector under a Gal-inducible promoter and transformed into the *trk1Δ:trk2Δ* yeast double mutant. The untransformed mutant cells only grow on high-K^+ medium (100 mM K^+) but not on low-K^+ medium (7 mM K^+) (Fig. 10). The transformants were selected on the high-K^+ medium (100 mM K^+) initially using the *URA3*-selectable marker and then transferred to the low-K^+ medium (7 mM K^+) containing Gal. Figure 10 shows that *KAT1** and *AKT1** transformants can grow on the low-K^+ medium, confirming previous reports (Anderson et al., 1992; Sentenac et al., 1992). However, *AKT2* transformants could not complement K^+ uptake into yeast even though AKT2 was transcribed, indicating that AKT2 is either not properly processed in yeast or incapable of restoring K^+ uptake (Fig. 10, four separate transformation experiments).

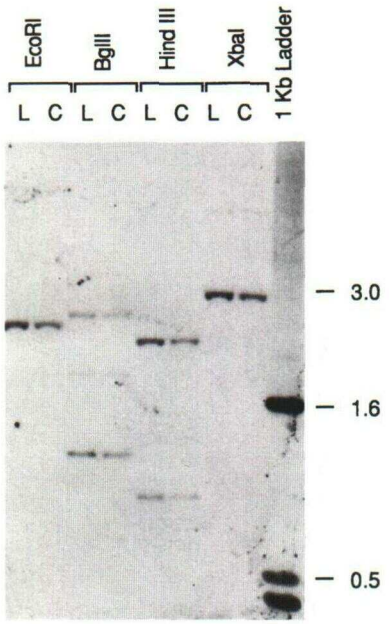

Figure 8. Genomic Southern analysis of the *AKT2* gene. Four micrograms of genomic DNA from Arabidopsis ecotypes Columbia (C) and Landsberg (L) were digested with *Eco*RI, *Bgl*II, *Hin*dIII, and *Xba*I. The blot was hybridized with the ^{32}P-radiolabeled *AKT2* cDNA probe. DNA length markers (1-kb Ladder) are given at right in kilobases.

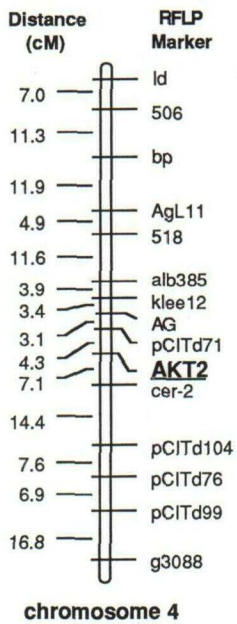

Figure 9. RFLP mapping of the *AKT2* gene. Chromosome localization of RFLP marker genes and the *AKT2* gene are shown. The numbers at left indicate the map distance (in centimorgans) between markers.

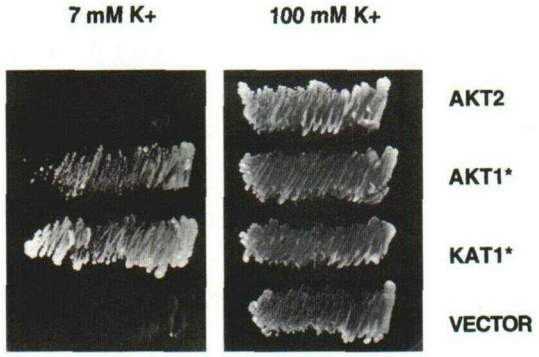

Figure 10. Complementation test in mutant yeast cells. Mutant *S. cerevisiae* cells (CY162) deleted for both *TRK1* and *TRK2* genes were transformed with the *KAT1**, *AKT1**, and *AKT2* genes or with the empty vector (pSE936). The transformants were streaked onto yeast nitrogen base medium without uracil (bottom), which contained approximately 7.7 mM K^+, or onto yeast nitrogen base medium without uracil supplemented with 100 mM KCl (top). Both media contained 2% Suc and 2% Gal.

The *AKT2* cDNA was also subcloned into the pBluescript KS vector for *Xenopus* oocyte expression. Injection of in vitro transcribed *AKT2* mRNA into *Xenopus* oocytes did not induce any exogenous current upon membrane depolarization or hyperpolarization. Furthermore, neither the *AKT2* nor the *AKT1** mRNAs increased linear leakage currents in oocytes as judged by oocyte background resistance measurements between −140 and +60 mV ($n > 200$ *AKT2*-injected oocytes; $n > 50$ *AKT1**-injected oocytes). Furthermore, we subcloned the *AKT2* cDNA into a baculovirus vector (pBlueBacIII) and generated recombinant viruses that harbor the *AKT2* coding sequence and can be infected into insect sf9 cells for high levels of expression. Whole-cell patch-clamp recordings of both uninfected and *AKT2*-infected sf9 cells revealed that the sf9 cells used in this study had an endogenous inward-rectifying current (Y. Cao, C. Schmidt, and J. I. Schroeder, unpublished results) and that *AKT2* infection did not induce any clearly discernible additional current or increase the endogenous inward-rectifying current.

DISCUSSION

Using low-stringency cDNA library screening, we isolated a novel cDNA, *AKT2*, from Arabidopsis. This new sequence shows a region with six putative transmembrane domains and a K^+-selective pore sequence (H5) between the fifth and sixth domains. These two sequence characteristics have previously been used as sufficient evidence to predict newly sequenced cDNAs as encoding K^+ channels (Milkman, 1994). Furthermore, the *AKT2* sequence shows highest similarity to the two known K^+ channel clones *KAT1* and *AKT1* (59–63% identity). Thus, we conclude that the *AKT2* clone is most likely a K^+ channel clone and that a multigene family of K^+ channels exists in the Arabidopsis genome. In animal systems, multigene families are a common feature of K^+ channels and are believed to be one of the mechanisms for generating functionally diversified K^+ channels (Chandy et al., 1990; Wei et al., 1990).

Expression Level-Induced Modulation of KAT1 Channel

The differences between the two K^+ currents induced by expression of *KAT1* mRNA and *KAT1** mRNA in *Xenopus* oocytes indicate interesting electrical properties of plant K^+ channels. Among the observed differences are the threshold of activation, the half-activation time, and the current amplitude. Western blot experiments directly demonstrated that the KAT1 protein is more abundant in *KAT1**-injected oocytes than in *KAT1*-injected oocytes (Fig. 4). Thus, the increase in the current amplitude in *KAT1**-injected oocytes can be ascribed to the higher level of expression. However, changes in half-activation times cannot be ascribed solely to this higher level of expression, because half-activation times reflect intrinsic biophysical properties of ion channels. Very et al. (1994) independently also reported effects of the quantity of KAT1 mRNA injection on half-activation times and further implicated a difference in channel sensitivity to Cs^+ blockage.

The observed shift in activation potential may have important implications for physiological functions of plant K^+ channels. For example, second-messenger inhibition of this class of K^+_{in} channels in guard cells has been shown to be accompanied by a hyperpolarizing shift in activation (Schroeder and Hagiwara, 1989; Fairley-Grenot and Assmann, 1991; Hoshi, 1995). (Note that the recently calculated 50% activation of −120 to −130 mV for KAT1 expressed in oocytes [Bertl et al., 1995] could not be confirmed for either the KAT1 or the KAT1* constructs analyzed here or previously [Schachtman et al., 1992]). Half-activation potentials of plant K^+_{in} do not shift significantly in response to extracellular K^+ changes (Thiel et al., 1992). However, the activation potentials do show small shifts to more negative potentials upon lowering external K^+ to <10 mM (Schroeder and Fang, 1991). These negative shifts in activation are unequivocally evident, because they physiologically prohibit large steady-state K^+ efflux currents that would otherwise be observed via K^+_{in} channels with 0 external K^+ or when the K^+ equilibrium potential is more negative than approximately −100 mV (Schroeder and Fang, 1991) (Fig. 2b, KAT1*). The differential effects of external K^+ on activation and half-activation parameters support the function of K^+_{in} channels for low-affinity K^+ uptake at physiological membrane potentials (Schroeder and Fang, 1991).

We can suggest several explanations to account for the differences in biophysical properties of K^+ channels at different expression levels. Overexpression could saturate posttranscriptional modification reactions that regulate channel properties, such as RNA editing, phosphorylation, or channel-channel interactions. For example, ATP and other cellular factors modulate KAT1 activation (Hoshi, 1995). Channel molecules may interact cooperatively at high packing density. Intermolecular cooperativity in biological membranes has been suggested for many animal receptors and ion channels (Hymel et al., 1988; Taleb and Betz, 1994), including voltage-gated K^+ channels (Honore et al., 1992; Moran et al., 1992), and has been recently suggested for a plant anion channel (Schmidt and Schroeder, 1994). In addition, clustering of high densities of channel proteins is well known in animal cells and has been shown to require cytoskeletal elements for localization and stabilization (Cooper, 1987; Grimminger et al., 1991; Peter et al., 1991). Furthermore, it has been suggested that Na^+ channels expressed in *Xenopus* oocytes form "hot spots," which reflect high channel densities (Stühmer et al., 1989). Such clustering phenomena would not be surprising for plant channels, because plant transport processes often require a polar localization in the plasma membrane. The observation that the KAT1* channel activates at a more positive potential indicates that plant K^+ channel expression levels may provide an additional mechanism for K^+ channel modulation. Furthermore, KAT1* activation properties may be relevant for K^+_{in} channel activation in vivo, since the activation potential for KAT1* is closer to the values recorded for some native plant cells under similar recording conditions and with similar external K^+ concentrations (Schroeder et al., 1987; Bush et al., 1988; Schroeder and Fang, 1991) and the estimated K^+_{in} densities of KAT1* are more similar to those observed in higher plant cells.

Posttranscriptional modification or significant structural changes may occur in KAT1, because a change in Cs^+ block has been implicated in dependence of the amount of KAT1 mRNA injected into oocytes (Very et al., 1994). A change in Cs^+ block would require a significant structural change in the pore structure of KAT1, which is also supported by putative differences in NH_4^+ selectivities demonstrated in oocytes (Schachtman et al., 1992) and estimated in yeast (Bertl et al., 1995) and differences in single-channel conductances obtained for KAT1 (28 ± 7 pS; Schachtman et al., 1992) and for KAT1* of 5 to 6 pS in 115 mM KCl (Hoshi, 1995; W. Gassmann and J. I. Schroeder, unpublished results). Note that the analysis of stretch channels in oocytes (Methfessel et al., 1986) was controlled for in membrane patches, which were used for single-channel KAT1 analysis, by applying suction and pressure to all membrane patches and selecting patches with channel currents that did not show regulation by membrane stretch (Schachtman et al., 1992) and that differed from stretch channel properties found in other patches, although spontaneous activity could not be ruled out. Analysis is furthur complicated by the presence of endogenous 5-pS channels. It is interesting that single-channel conductances of native K^+_{in} channels in higher plant cells also vary considerably from approximately 5 to 40 pS in 100 mM K^+ (for review and more complete refs., see Schroeder et al., 1994). Therefore, either endogenous oocyte ion channels or posttranscriptional modifications may produce the apparent variation of KAT1 conductances. The large differences in K^+_{in} conductances in plant cells suggest that small structural changes can greatly influence the single-channel conductance parameter of plant K^+ channels, which alone would unlikely be of physiological significance because of the high transport rate and sufficient density of channels. However, the accompanying macroscopic differences in K^+ channel properties reported here and elsewhere (Very et al., 1994; Hoshi, 1995) would be of physiological importance. Elucidation of the structural basis for posttranscriptional changes in KAT1 properties will require further investigation.

The cation selectivity of KAT1 (Schachtman et al., 1992; Very et al., 1995) and KAT1*, as determined by current amplitudes at −120 mV in the presence of 115 mM K^+ and other monovalent cations, was comparable within the derived statistical variations. NH_4^+ to K^+ current magnitude ratios were 28% for KAT1*, which correlates with 30% for KAT1 (Schachtman et al., 1992), and are comparable to values from native K^+_{in} channels as studied in plant cells (Gassmann and Schroeder, 1994). These data quantitatively differ from an NH_4^+ to K^+ conductance ratio of KAT1 determined in yeast of 5%, which requires subtraction of endogenous hyperpolarization-activated NH_4^+ currents measured in separate non-KAT1-expressing yeast cells (Bertl et al., 1995). In contrast to a proposed hypothesis (Bertl et al., 1995), oocytes used in this and previous studies have small, linear NH_4^+ currents, which do not show hyperpolarization-induced time-dependent activation. Correction for linear background conductances, as described previously (Cao et al., 1992; Schachtman et al., 1992), therefore allows accurate determination of NH_4^+ selectivity in oocytes (Schachtman et al., 1992; Uozumi et al., 1995). Furthermore, single-point mutations in KAT1 can convert KAT1 from a K^+ over NH_4^+-selective channel to a channel that shows a high selectivity for NH_4^+ over K^+ of approximately 10 to 1 (Uozumi et al., 1995). These data further support the NH_4^+ permeability of KAT1. Note that influx of NH_4^+ into yeast is most likely to cause large acidification in cytosolic pH, because of the large membrane surface to volume ratio; acidification in turn reduces KAT1 currents (Hoshi, 1995). The question of whether the NH_4^+ selectivity of KAT1 expressed in yeast has a difference from that demonstrated in oocytes (Schachtman et al., 1992) could be addressed by pH buffering and/or by expression of KAT1 in available yeast mutants with disrupted NH_4^+ uptake transporters.

Structural Features and Functional Implications of Plant K^+ Channels

The three plant K^+ channel genes *KAT1*, *AKT1*, and *AKT2* share significant sequence homology, particularly in the hydrophobic core region (S1–S6). Within this region, the levels of amino acid identities are high, ranging from 59 to 63% (Table I). The levels of amino acid identities among the four subfamilies (*Shak*, *Shab*, *Shaw*, and *Shal*) of K^+_{out} channels in animals are significantly smaller (38–45%, Table I), but higher levels of approximately 70% are found among members of each subfamily (Jan and Jan, 1992). These results suggest that the three plant K^+ channel genes might be functionally closely related. However, when the three genes were transformed into a yeast mutant defective in K^+ uptake, only *KAT1* and *AKT1* complement the mutation (Anderson et al., 1992; Sentenac et al., 1992; Fig. 10), whereas *AKT2* did not complement K^+ uptake. Furthermore, only KAT1 was functional in oocytes, whereas neither AKT1 ($n > 50$ oocytes, data not shown) nor AKT2 alone or when expressed simultaneously produced significant currents in oocytes. It is possible that the AKT2 protein is not synthesized or processed properly in yeast or in oocytes or is not correctly targeted to the plasma membrane. However, other possibilities may also exist. For example, a modification event such as protein phosphorylation or nucleotide binding may be required for channel function in yeast or in oocytes. *AKT2* may encode a K^+_{out} channels in view of the charge differences in the putative S4 voltage-sensing sequence (Fig. 6a) and in other sequences between *AKT2* and the other two plant channels. A K^+_{out} channel would not complement the K^+ uptake deficiency of the yeast *trk1:trk2* mutant. More detailed biophysical and biochemical analyses of these proteins expressed in systems such as plant cells, yeast, *Xenopus* oocytes, or insect cells and immunochemical analyses with antibodies specifically against AKT2 and AKT1 proteins will be required to differentiate among these possibilities and to assign specific functions to each of the proteins.

It is interesting that the three cloned Arabidopsis K^+ channel genes display remarkably different expression patterns. *AKT2* is expressed at high levels in leaf tissues, whereas *AKT1* is mainly expressed in root tissues (Fig. 7). *KAT1* is much less abundant in these two tissue types and could not be detected on our northern blots. This differential expression pattern indicates different roles of K^+ channels in various tissues and during plant growth and development.

K^+ transport in leaves is of central significance for important plant physiological processes such as leaf expansion and photosynthetic homeostasis (Behboudian and Anderson, 1990; Antonenko et al., 1994; Elzenga and Van Volkenburgh, 1994). The high level of *AKT2* expression in leaves indicates that this novel K^+ channel cDNA may contribute to physiological K^+ transport in leaves. Molecular biological and genetic analyses will be helpful for further understanding the function of this channel.

In conclusion, plant K^+ channels are encoded by multiple genes and are differentially expressed in leaves and roots. Heterologous expression analyses show that the expression level of *KAT1* is an important factor in determining activation properties of plant K^+_{in} channels. Since *AKT1* is predominantly expressed in roots and *AKT2* is highly expressed in leaves, further studies should provide information regarding the physiological functions of these K^+ channels in whole plants.

ACKNOWLEDGMENTS

For providing the *XSha2* cDNA clone, we thank Dr. N. Spitzer at the University of California, San Diego. We also thank Dr. C. Labarca (California Institute of Technology, Pasadena) for the pBS-KS$^+$AMV-pA50 vector, Dr. M. Yanofsky and Ms. S. Kempin (University of California, San Diego) for help with RFLP mapping of the *AKT2* clone, Dr. Y-F. Tsay for the Arabidopsis mRNA, and Walter Gassmann for comments concerning the manuscript.

Received July 3, 1995; accepted July 30, 1995.

LITERATURE CITED

Anderson JA, Huprikar SS, Kochian LV, Lucas WJ, Gaber RF (1992) Functional expression of a probable *Arabidopsis thaliana* potassium channel in *Saccharomyces cerevisiae*. Proc Natl Acad Sci USA **89:** 3736–3740

Antonenko YN, Rokitskaya TI, Kotova EA, Taisova AS (1994) Ionic channel activity induced by fusion of *Rhodospirillum rubrum* chromatophores with a planar bilayer lipid membrane. FEBS Lett **337:** 77–80

Baines AB (1990) Ankyrin and the node of ranvier. Trends Neurosci **13:** 119–121

Behboudian MH, Anderson DR (1990) Effects of potassium deficiency on water relations and photosynthesis of the tomato plant. Plant Soil **127:** 137–139

Bennett V (1992) Ankyrins. J Biol Chem **267:** 8703–8706

Bertl A, Anderson JA, Slayman CL, Gaber RF (1995) Use of *Saccharomyces cerevisiae* for patch-clamp analysis of heterologous membrane proteins: characterization of Kat1, an inward-rectifying K^+ from *Arabidopsis thaliana*, and comparison with endogenous yeast channels and carriers. Proc Natl Acad Sci USA **92:** 2701–2705

Bezanilla F, Armstrong CM (1977) Inactivation of the sodium channel. I. Sodium current experiments. J Gen Physiol **70:** 549–566

Brown AM (1993) Functional bases for interpreting amino acid sequences of voltage-dependent K^+ channels. Annu Rev Biophys Biomol Struct **22:** 173–198

Bush DS, Hedrich R, Schroeder JI, Jones RL (1988) Channel-mediated K^+ flux in barley aleurone protoplasts. Planta **176:** 368–377

Cao Y, Anderova M, Crawford NM, Schroeder JI (1992) Expression of an outward rectifying potassium channel from maize mRNA and complementary RNA in *Xenopus* oocytes. Plant Cell **4:** 961–969

Cao Y, Crawford NM, Schroeder JI (1995) Amino terminus and the first four membrane-spanning segments of the *Arabidopsis* K^+ channel KAT1 confer inward-rectification property of plant animal chimeric channels. J Biol Chem **270:** 17697–17701

Chandy KG, Williams CB, Spencer RH, Aguilar BA, Ghanshani S, Tempel BL, Gutman GA (1990) A family of three mouse potassium channel genes with intronless coding regions. Science **247:** 973–975

Chang C, Bowman JL, DeJohn AW, Lander ES, Meyerowitz EM (1988) Restriction fragment length polymorphism linkage map for *Arabidopsis thaliana*. Proc Natl Acad Sci USA **85:** 6856–6860

Cooper JA (1987) Effects of cytochalasin and phalloidin on actin. J Cell Biol **105:** 1473–1478

Corey JL, Davidson N, Lester H, Brecha N, Quick MW (1994) Protein kinase C modulates the activity of a cloned γ-aminobutyric acid transporter expressed in *Xenopus* oocytes via regulated subcellular redistribution of the transporter. J Biol Chem **269:** 14759–14767

Dohmen RJ, Strasser AW, Honer CB, Hollenberg CP (1991) An efficient transformation procedure enabling long-term storage of competent cells of various yeast genera. Yeast **7:** 691–692

Drain P, Dubin AE, Aldrich RW (1994) Regulation of *Shaker* K^+ channel inactivation gating by the cAMP-dependent protein kinase. Neuron **12:** 1097–1109

Elledge SJ, Mullagin JT, Ramer SW, Spottswood M, Davis RW (1991) λYES: a multifunctional cDNA expression vector for the isolation of genes by complementation of yeast and *Escherichia coli* mutations. Proc Natl Acad Sci USA **88:** 1731–1734

Elzenga JT, Van Volkenburgh E (1994) Characterization of ion channels in the plasma membrane of epidermal cells of expanding pea (*Pisum sativum* arg) leaves. J Membr Biol **137:** 227–235

Fairley-Grenot KA, Assmann SM (1991) Evidence for G-protein regulation of inward K^+ channel current in guard cells of fava bean. Plant Cell **3:** 1037–1044

Fairley-Grenot KA, Assmann SM (1993) Comparison of K^+-channel activation and deactivation in guard cells from a dicotyledon (*Vicia faba* L.) and a graminaceous monocotyledon (*Zea mays*). Planta **189:** 410–419

Gassmann W, Schroeder JI (1994) Inward-rectifying K^+ channels in root hairs of wheat. A mechanism for aluminum-sensitive low-affinity K^+ uptake. Plant Physiol **105:** 1399–1408

Grimminger F, Sibelius U, Aktories K, Just I, Seeger W (1991) Suppression of cytoskeletal rearrangement in activated human neutrophils by botulinum C2 toxin: impact on cellular signal transduction. J Biol Chem **266:** 19276–19282

Hanley BA, Schuler MA (1988) Plant intron sequences: evidence for distinct groups of introns. Nucleic Acids Res **16:** 7159–7175

Ho K, Nichols CG, Lederer WJ, Lytton J, Vassilev PM, Kanazirska MV, Hebert SC (1993) Cloning and expression of an inwardly rectifying ATP-regulated potassium channel. Nature **362:** 31–38

Hoger JH, Walter AE, Vance D, Yu L, Lester HA, Davidson N (1991) Modulation of a cloned mouse brain potassium channel. Neuron **6:** 227–236

Honore E, Attali B, Romey G, Lesage F, Barhanin J, Lazdunski M (1992) Different types of K^+ channel current are generated by different levels of a single mRNA. EMBO J **11:** 2465–2471

Hoshi T (1995) Regulation of voltage dependence of the KAT1 channel by intracellular factors. J Gen Physiol **105:** 309–320

Hymel L, Streissing J, Glossmann H, Schindler H (1988) Purified skeletal muscle 1,4-dihydropyridine receptor forms phosphorylation-dependent oligomeric calcium channels in planar bilayers. Proc Natl Acad Sci USA **85:** 4290–4294

Isacoff EY, Jan YN, Jan LY (1990) Evidence for the formation of heteromultimeric potassium channels in *Xenopus* oocytes. Nature **345:** 530–534

Jan LY, Jan YN (1992) Structural elements involved in specific K^+ channel functions. Annu Rev Physiol **54:** 537–555

Joshi CP (1987) An inspection of the domain between putative TATA box and translation start site in 79 plant genes. Nucleic Acids Res **15:** 6643–6651

Kaupp UB, Niidome T, Tanabe T, Terada S, Bonigk W, Stuhmer W, Cook NJ, Kangawa K, Matsuo H, Hirose T, Mayata T, Numa S (1989) Primary structure and functional expression from complementary DNA of the rod photoreceptor cyclic GMP-gated channel. Nature **342:** 762–766

Ko CH, Gaber RF (1991) TRK1 and TRK2 encode structurally related K^+ transporters in *Saccharomyces cerevisiae*. Mol Cell Biol **8:** 4266–4273

Kochian LV, Garvin DF, Shaff JE, Chilcott TC, Lucas WJ (1993) Towards an understanding of the molecular basis of plant K^+ transport: characterization of cloned K^+ transport cDNAs. Plant Soil **155/156:** 115–118

Kochian LV, Lucas WJ (1988) Potassium transport in roots. Adv Bot Res **15:** 93–177

Kozak M (1989) The scanning model for translation: an update. J Cell Biol **108:** 229–241

Kubo Y, Baldwin TJ, Jan YN, Jan LY (1993a) Primary structure and functional expression of a mouse inward rectifier potassium channel. Nature **362:** 127–133

Kubo Y, Reuveny E, Slesinger PA, Jan YN, Jan LY (1993b) Primary structure and functional expression of a rat G-protein-coupled muscarinic potassium channel. Nature **364:** 802–806

Kyte J, Doolittle RF (1982) A simple method for displaying the hydropathic character of a protein. J Mol Biol **157:** 105–132

Laemmli UK (1970) Cleavage of structural proteins during the assembly of the head of bacteriophage T_4. Nature **227:** 680–685

Lander LRR, Green MP, Abrahamson J, Barlow A, Dale M, Lincoln SE, Newsburg L (1987) MAPMAKER: an interactive computer package for constructing primary genetic linkage maps of experimental and natural populations. Genomics **1:** 174–181

Lew RR (1991) Electrogenic transport properties of growing *Arabidopsis* root hairs. The plasma membrane proton pump and potassium channels. Plant Physiol **97:** 1527–1534

Lux SE, John KM, Bennett V (1990) Analysis of cDNA for human erythrocyte ankyrin indicates a repeated structure with homology to tissue-differentiation and cell-cycle control proteins. Nature **344:** 36–42

Methfessel C, Witzemann V, Takahashi T, Mishina M, Numa S, Sakmann B (1986) Patch clamp measurements on *Xenopus laevis* oocytes: currents through endogenous channels and implanted acetylcholine receptor and sodium channels. Pflueger Arch **407:** 577–588

Milkman R (1994) An *Escherichia coli* homologue of eukaryotic potassium channel proteins. Proc Natl Acad Sci USA **91:** 3510–3514

Moran N, Satter RL (1989) K^+ channels in plasmalemma of motor cells of *Samanea saman*. *In* J Dainty, MID Michelis, E Marré, F Rasi-Coldogno, eds, Plant Membrane Transport. Elsevier, Amsterdam, The Netherlands, pp 529–530

Moran O, Schreibmayer W, Weigl L, Dascal N, Lotan I (1992) Level of expression controls modes of gating of a K^+ channel. FEBS Lett **302:** 21–25

Perozo E, Bezanilla F (1990) Phosphorylation affects voltage gating of the delayed rectifier K^+ channel by electrostatic interactions. Neuron **5:** 663–674

Peter AB, Schittny JC, Niggli V, Reuter H, Sigel E (1991) The polarized distribution of poly(A)$^+$-mRNA-induced functional ion channels in the *Xenopus* oocyte plasma membrane is prevented by anticytoskeletal drugs. J Cell Biol **114:** 455–464

Ramos J, Contreras P, Rodriguez-Navarro A (1985) A potassium transport mutant of *Saccharomyces cerevisiae*. Arch Microbiol **143:** 88–96

Rettig J, Heinemann SH, Wunder F, Lorra C, Parcej DN, Dolly JO, Pongs O (1994) Inactivation properties of voltage-gated K^+ channels altered by presence of beta-subunit. Nature **369:** 289–294

Ribera AB (1990) A potassium channel gene is expressed at neural induction. Neuron **5:** 691–701

Rüppersberg JP, Schroter KH, Sakmann B, Stocker M, Sewing S, Pongs O (1990) Heteromultimeric channels formed by rat brain potassium channel proteins. Nature **345:** 535–537

Schachtman DP, Schroeder JI, Lucas WJ, Anderson JA, Gaber RF (1992) Expression of an inward-rectifying potassium channel by the *Arabidopsis KAT1* cDNA. Science **258:** 1654–1658

Schmidt C, Schroeder JI (1994) Anion selectivity of slow anion channels in the plasma membrane of guard cells. Large nitrate permeability. Plant Physiol **106:** 383–391

Schroeder JI (1988) K^+ transport properties of K^+ channels in the plasma membrane of *Vicia faba* guard cells. J Gen Physiol **92:** 667–683

Schroeder JI (1995) Magnesium-independent activation of inward-rectifying K^+ channels in *Vicia faba* guard cells. FEBS Lett **363:** 157–160

Schroeder JI, Fang HH (1991) Inward-rectifying K^+ channels in guard cells provide a mechanism for low-affinity K^+ uptake. Proc Natl Acad Sci USA **88:** 11583–11587

Schroeder JI, Hagiwara S (1989) Cytosolic calcium regulates ion channels in the plasma membrane of *Vicia faba* guard cells. Nature **338:** 427–430

Schroeder JI, Hedrich R (1989) Involvement of ion channels and active transport in osmoregulation and signaling of higher plant cells. Trends Biochem Sci **14:** 187–192

Schroeder JI, Raschke K, Neher E (1987) Voltage dependence of K^+ channels in guard-cell protoplasts. Proc Natl Acad Sci USA **84:** 4108–4112

Schroeder JI, Ward JM, Gassmann W (1994) Perspectives on the physiology and structure of inward-rectifying K^+ channels in higher plants: biophysical implications for K^+ uptake. Annu Rev Biophys Biomol Struct **23:** 441–471

Schwarz TL, Tempel BL, Papazian DM, Jan YN, Jan LY (1988) Multiple potassium-channel components are produced by alternative splicing at the *shaker* locus in *Drosophila*. Nature **331:** 137–142

Sentenac H, Bonneaud N, Minet M, Lacroute F, Salmon JM, Gaymard F, Grignon C (1992) Cloning and expression in yeast of a plant potassium ion transport system. Science **256:** 663–665

Simons PJ (1981) The role of electricity in plant movements. New Phytol **87:** 11–37

Spalding EP, Goldsmith MHM (1993) Activation of K^+ channels in the plasma membrane of *Arabidopsis* by ATP produced photosynthetically. Plant Cell **5:** 477–484

Stühmer W, Conti F, Suzuki H, Wang X, Noda M (1989) Structural parts involved in activation and inactivation of sodium channel. Nature **339:** 597–603

Sussman MR (1992) Shaking *Arabidopsis thaliana*. Science **256:** 619

Taleb O, Betz H (1994) Expression of the human glycine receptor a1 subunit in *Xenopus* oocytes: apparent affinities of agonists increase at high receptor density. EMBO J **13:** 1318–1324

Tempel BL, Papazian DM, Schwarz TL, Jan YN, Jan LY (1987) Sequence of a probable potassium channel component encoded at *Shaker* locus of *Drosophila*. Science **237:** 770–775

Tester M (1990) Plant ion channels: whole-cell and single-channel studies. New Phytol **114:** 305–340

Thiel G, MacRobbie EAC, Blatt MR (1992) Membrane transport in stomatal guard cells: the importance of voltage control. J Membr Biol **126:** 1–18

Tsay YF, Schroeder JI, Feldmann KA, Crawford NM (1993) The herbicide sensitivity gene *CHL1* of *Arabidopsis* encodes a nitrate-inducible nitrate transporter. Cell **72:** 705–713

Uozumi N, Gassmann W, Cao Y, Schroeder JI (1995) Identification of strong modifications in cation selectivity in an *Arabidopsis* inward rectifying potassium channel by mutant selection in yeast. J Biol Chem **270:** 24276–24281

Very AA, Bosseux C, Gaymard F, Sentenac H, Thibaud JB (1994) Level of expression in *Xenopus* oocytes affects some characteristics of a plant inward-rectifying voltage-gated K^+ channel. Pflugers Arch **428:** 422–424

Very AA, Gaymard F, Bosseux C, Sentenac H, Thibaud JB (1995) Expression of a cloned plant K^+ channel in Xenopus oocytes: analysis of macroscopic currents. Plant J **7:** 321–332

Ward JM, Reinders A, Hsu H-T, Sze H (1992) Dissociation and reassembly of the vacuolar H^+-ATPase complex from oat roots. Plant Physiol **99:** 161–169

Warmke J, Drysdale R, Ganetzky B (1991) A distinct potassium channel polypeptide encoded by the *Drosophila eag* locus. Science **252:** 1560–1562

Weber IT, Steitz TA (1984) Model of specific complex between catabolite gene activator protein and B-DNA suggested by electrostatic complementarity. Proc Natl Acad Sci USA **81:** 3973–3977

Wei A, Covarrubias M, Butler A, Baker K, Pak M, Salkoff L (1990) K^+ current diversity is produced by an extended gene family conserved in *Drosophila* and mouse. Science **248:** 599–603

Wilkinson JQ, Crawford NM (1991) Identification of the *Arabidopsis CHL3* gene as the nitrate reductase structural gene *NIA2*. Plant Cell **3:** 461–471

Zhang H, Scheirer DC, Fowle WH, Goodman HM (1992) Expression of antisense or sense RNA of an ankyrin repeat-containing gene blocks chloroplast differentiation in *Arabidopsis*. Plant Cell **4:** 1575–1588